Electronic Supplementary Material (ESI) for Soft Matter

Supporting Information

Combining Metadynamics Simulation and Experiments to Characterize Dendrimers in Solution

Giovanni M. Pavan[,a,‡], Alessandro Barducci*[,b,c,‡], Lorenzo Albertazzi[d] and Michele Parrinello[b,c]*

[a] Department of Innovative Technologies, University of Applied Science of Southern Switzerland, Galleria 2, 6928 Manno, Switzerland. E-mail: giovanni.pavan@supsi.ch

[b] ETH Zurich, Department of Chemistry and Applied Biosciences, c/o USI Campus, Via Giuseppe Buffi 13, 6900 Lugano, Switzerland. E-mail: alessandro.barducci@phys.chem.ethz.ch

[c] Università della Svizzera Italiana, Facoltà di Informatica, Istituto di Scienze Computazionali, Via Giuseppe Buffi 13, 6900 Lugano, Switzerland

[d] Institute for Complex Molecular Systems and Laboratory of Macromolecular and Organic Chemistry, Eindhoven University of Technology, P.O. Box 513, 5600 MB, Eindhoven, The Netherlands

TABLE OF CONTENTS

Computational procedure

The construction and parametrization of the molecular models used in this study were carried out using the AMBER 11 suite of programs.[S1] The starting molecular model for the larger **G2-2kPEG** dendrimer was constructed as composed by different residues[S2] in accordance with our previous study on a fluorescent sensor built on this scaffold.[S3] The internal G2 PAMAM dendrimer was composed by a central (CEN) unit, the repetitive units that constitute the branched dendritic scaffold (BRA) and the 16 terminal surface groups (END). The dendrimer's surface amines were conjugated to 16 linear PEG chains composed by 44 PolyEthilene Glycol (PEG) monomers each (molecular weight of each PEG chain: 2 kDa).[S3,S4] The starting configurations for **G2**, **G2+** and **G2-550PEG** were obtained respectively by deletion or shortening of the PEG chains of **G2-2kPEG** (12 PEG residues compose a single 550 Da PEG chain). At neutral pH (≈7.4) **G2-550PEG** and **G2-2kPEG** are both neutral. In the same condition, the surface amines of **G2+** are naturally protonated (NH_3^+), leading to a theoretical net charge of +16 e. The native dendrimer was studied also at high pH (>10). In this condition **G2** is uncharged and decorated by neutral NH_2 surface groups. The same conditions were also maintained in the DLS experiments for consistency.

All the non-standard residues composing the dendrimers were parametrized according to the validated procedure adopted by our group in previous studies on dendrimers[S2] and dendrons.[S5] The partial charges were obtained using the AM1-BCC[S6] calculation method within the *antechamber*[S7] module of AmberTools 1.4 (AMBER 11). Parameters and force field types were assigned consistently with the "general AMBER force field (GAFF)" (*gaff.dat*).[S8]

The dendrimers were solvated in a periodic box containing TIP3P water molecules[S9] extending 12 Å from the solute atoms. A suitable number of Cl^- and Na^+ ions were added in the system – using the *leap* module within AMBER 11 to reproduce the experimental ionic concentration of 150 mM NaCl. In particular, the ions were added in the periodic systems with the standard *addIons* utility of *leap* – i.e., they were placed onto a shell around the solute using a Coulombic potential on a grid.

Eventual superposing water molecules were replaced with ions. The *parm99* all-atom force field by Cornell et al.[S10] was used for the standard residues present in the systems.

After preliminary minimization, each of the three systems underwent 100 ns of well-tempered metadynamics simulation (WT-MetaD).[S11] All the simulation work was conducted using the NAMD 2.8 software[S12] and the PLUMED 1.3 plugin.[S13] The WT-MetaD simulations were conducted in NPT periodic boundary condition at temperature of 300 K and pressure of 1 atm, using a time step of 2 femtoseconds, the Langevin thermostat and a 8 Å cutoff. The particle mesh Ewald[S14] (PME) approach was used to treat the long-range electrostatic effects and the RATTLE algorithm was used on the bonds involving Hydrogen atoms. [S15]

The radius of gyration (R_g) and the coordination between the PEG atoms were used as collective variables (CV1 and CV2 respectively) – i.e., as descriptors of the behavior of these molecules in solution. In PLUMED 1.3,[S13] CV1 (radius of gyration) is expressed according to Eq. S1:

$$s_{gyr} = \sqrt[2]{\frac{\sum_i^n |r_i - r_{COM}|^2}{\sum_i^n m_i}} \qquad \text{(S1 - CV1)}$$

where the center of mass is defined as:

$$r_{COM} = \frac{\sum_i^n r_i m_i}{\sum_i^n m_i} \qquad \text{(S2)}$$

After a first trial phase where the simulation parameters were tuned properly, the gaussian SIGMA for CV1 was set to 0.1 Å for **G2**, **G2+** and **G2-550PEG**, and to 0.15 Å for **G2-2kPEG** respectively. A HILLS height of 0.6 kcal mol^{-1} was used in all cases. Upper wall limit for the CV1 (R_g) variable were fixed to 21.0 Å and 42.0 Å for **G2-550PEG** and **G2-2kPEG** respectively, as it was evident that higher Rg values were not energetically accessible. No upper wall limit for the CV1 variable was used for **G2** and **G2+**.

The coordination number collective variable (COORD – CV2) to count the total number of contacts between atoms in the group A with those in the group B is defined as:

$$s_{coord} = \sum_{i \in A} \sum_{j \in B} s_{ij} \qquad \text{(S3 – CV2)}$$

Where the individual contributions s_{ij} are defined as:

$$s_{ij} = \begin{cases} 1 & \text{for } r_{ij} = 0 \\ \frac{1-\left(\frac{r_{ij}}{r_0}\right)^n}{1-\left(\frac{r_{ij}}{r_0}\right)^m} & \text{for } r_{ij} > 0 \end{cases} \quad \text{(S4)}$$

and where:

$$r_{ij} = \left|r_i - r_j\right| \quad \text{(S5)}$$

In this case, groups A and B are coincident as CV2 was defined as the number of contacts of PEG atoms with themselves. The values of the r_0, n and m parameters were thus fixed to 7.5, 6 and 10 respectively. The gaussian SIGMA for CV2 were set to 25.0 and 50.0 for **G2-550PEG** and **G2-2kPEG** respectively. Due to the consistent computational effort required for these kind of simulations, while for **G2-550PEG** all of the PEG Oxygen atoms were considered for CV2, this number was reduced to one PEG Oxygen every two for the larger **G2-2kPEG**. For the WT-MetaD simulations of **G2** and **G2+** CV2 was not used as PEG was not present.

The free energy surfaces (FESs) were obtained from the WT-MetaD trajectories as calculated respect to R_g and the number of contacts between PEG's atoms (these additional FES plots for **G2-550PEG** and **G2-2kPEG** are reported in Figure S1). Data extracted from the WT-MetaD trajectories were also processed and reweighted[S16] further in order to obtain the free energy surfaces (FES) calculated with respect to the molecular radius of gyration (R_g) and solvent accessible surface area (SASA), which provide a more transparent picture. Also in the case **G2**, where R_g was used as unique CV during the simulation, data from WT-MetaD simulation were reweighted to express the FES calculated as a function of R_g and SASA (see Figure S2).

The FES expressed as function of R_g and SASA identified clear minima for **G2-550PEG** and **G2-2kPEG** at low R_g and SASA values (see Figure 2 in the main paper). These minima indicate that at the equilibrium the dendrimers are folded. Two major minima with similar shape can be seen for both molecules – one lying between R_g≈14–17 Å and SASA≈8000–12000 Å^2 for **G2-550PEG**, and

another one for **G2-2kPEG** comprised between R_g≈23–25 Å and SASA≈19000–23000 Å^2. The same is true for **G2** – the FES in Figure S2 shows a minimum between R_g≈10–15 Å and SASA≈3000–4500 Å^2. The FES of **G2+** is different. The minimum is broader (R_g≈12–19.5 Å and SASA≈4000–5750 Å^2) the FES is smoother. This is consistent with a more open configuration of G2+ in solution and a higher flexibility due to the fact that the surface of **G2+** is charged. Since only the dark zones reported in the FES are energetically accessible (Figure 2, main text, and Figure S2 for **G2**), the WT-MetaD trajectories of all the molecules were processed with the CatDCD 4.0 plugin of VMD.[S17] All the configurations out of the minima were discarded and new trajectories collecting only the most energetically accessible configurations were obtained. These new minimum trajectories were used to calculate the molecular size, the theoretical density (according to a spherical model) and the water mass fraction absorbed by each dendrimer. These quantities were obtained using the *ptraj* module of AMBER 11.

The same minimum trajectories were used to compute the solvation energy (G_{sol}) of **G2**, **G2+**, **G2-550PEG** and **G2-2kPEG** with the *mm_pbsa.pl* module of AMBER 11 and according to the MM-PBSA approach.[S18] The solvation energies were obtained as $G_{sol} = G_{PB} + G_{NP}$,[S19] where the polar component of G_{PB} was evaluated using the Poisson-Boltzmann[S20] (PB) approach with a numerical solver implemented in the *pbsa* program of AMBER 11.[S21] The non-polar contribution to the solvation energy was calculated as $G_{NP} = \gamma$ (SASA) + β, in which γ = 0.00542 kcal/Å^2, β = 0.92 kcal/mol. The solvent-accessible surface data, SASA, used for the WT-MetaD reweighting were estimated for all the molecules with the MSMS program.[S22] Solvation energies were then normalized according to the molecular weight (Mw) of each molecule. Solvation and density data for **G2** and **G2+** are reported in Figure S2b and S3b.

Experimental procedure

The G2 ethylenediamine core PAMAM dendrimer was purchased from Sigma Aldrich and used without further purification. NHS-activated PEGs (MW=550 Da and MW=2 kDa) were purchased from Laysan Bio. The polydispersity index (PDI) for the PEG purchased from Laysan Bio does not exceed 1.05. The synthetic procedure and the characterization of G2 PAMAM-PEG conjugates have been previously reported by our group.[S3] For dynamic light scattering (DLS) measurements the pegylated dendrimers (**G2-550PEG** and **G2-2kPEG**) were dissolved in water with 150 mM NaCl at pH=7.4. Since we were interested in the study of the influence of different pegylation on the dendrimers hydrophilicity, G2 PAMAM dendrimer was measured both at neutral (≈7.4 – **G2+**) and high pH (≈10 – **G2**). DLS measurements were obtained by means of a Zetasizer Nano ZS90 (Malvern Instruments) equipped with a He-Ne 633 nm laser. The temperature in the cell compartment was set to 300 K.

Additional FES plots and size data for G2, G2+, G2-550PEG and G2-2kPEG

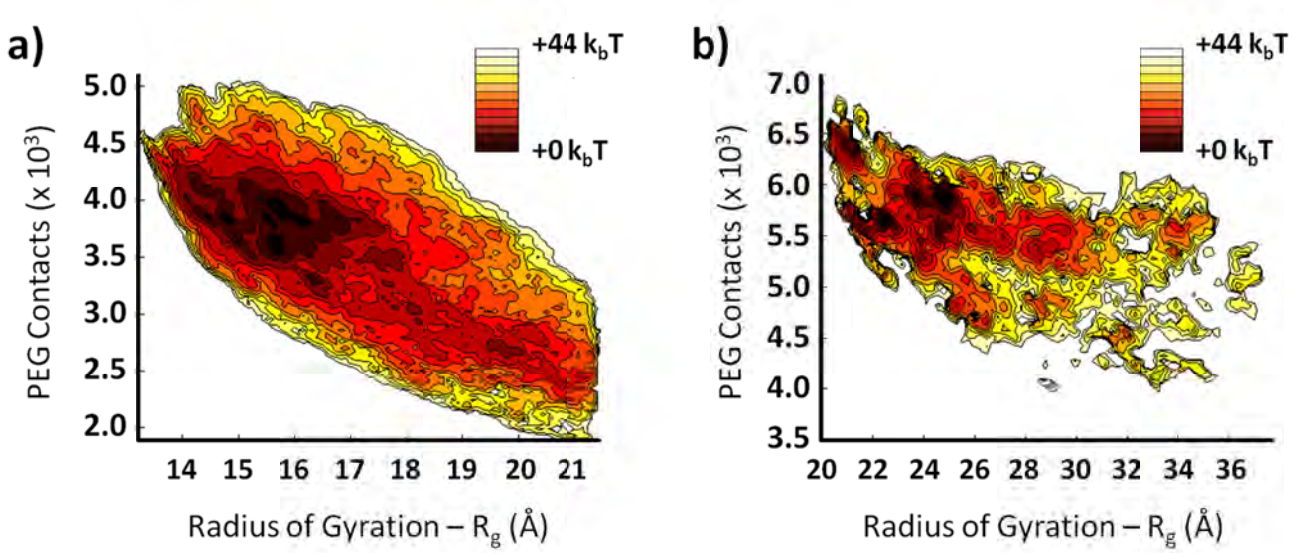

Figure S1. The free energy surfaces (FES) of **G2-550PEG** (a) and **G2-2kPEG** (b) obtained from WT-MetaT simulations and calculated with respect to PEG Oxygen atoms coordination (number of contacts: *y* axis) and radius of gyration (R_g – *x* axis). Isolines identify free energy differences of 4 k_bT. The darkest the FES region are the most energetically accessible, and are representative of the most probable molecular configurations. In the count of PEG coordination (*y* axis) all the PEG Oxygens were considered for **G2-550PEG,** while the atom number was decreased to one Oxygen every two in the case of **G2-2kPEG** (b).

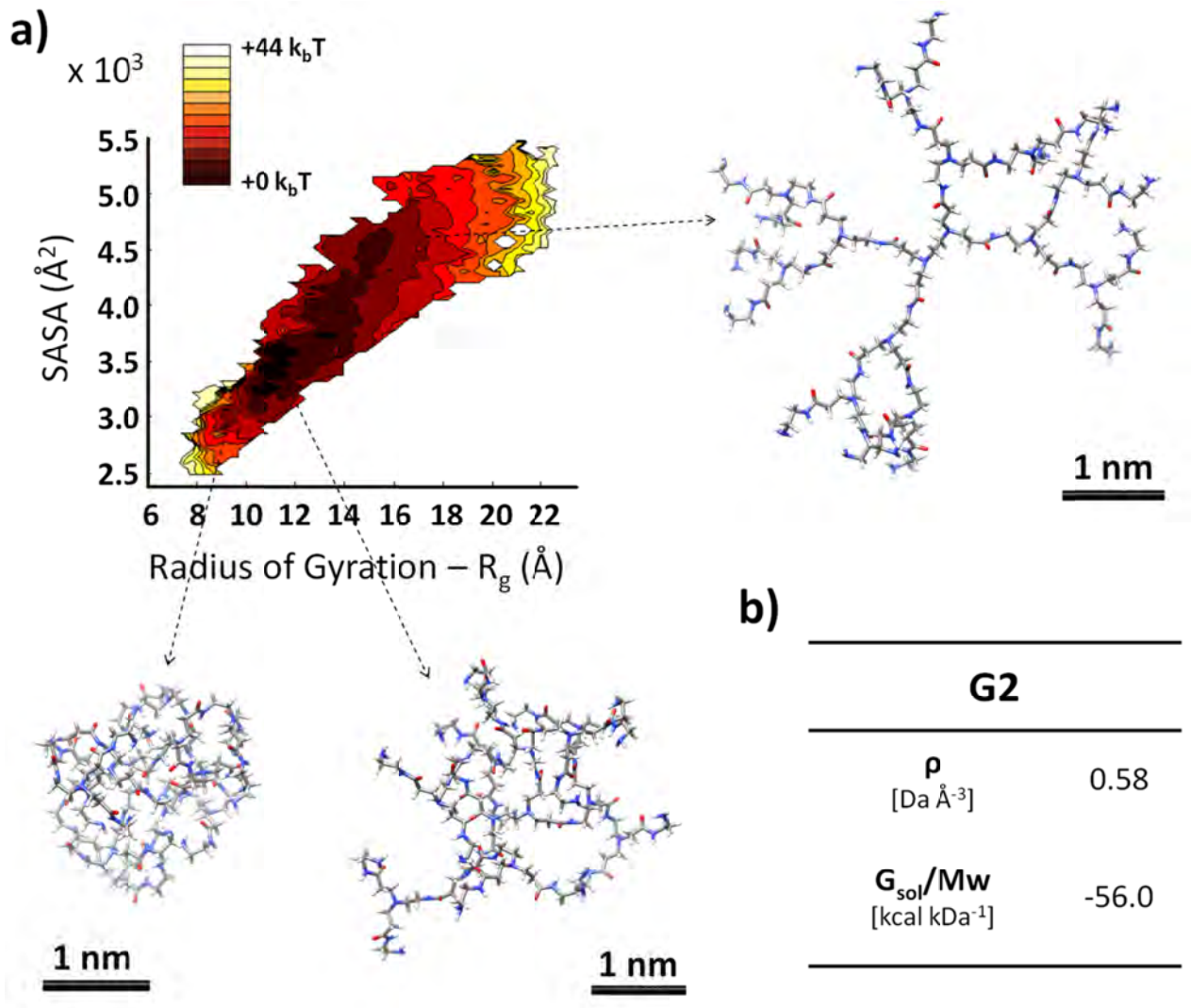

Figure S2. The free energy surfaces (FES**)** of **G2** (a) obtained from WT-MetaT simulations and calculated respect solvent accessible surface area (SASA – *y* axis) and radius of gyration (R_g – *x*

axis). Isolines identify free energy differences of 4 k_bT. The darkest the FES region are the most energetically accessible, and are representative of the most probable molecular configurations. The dendrimer is colored by atom (C: grey, O: red, N: blue and H: white). Explicit water molecules and Cl^- and Na^+ ions are not shown for clarity. Density and solvation energy data for **G2** for the configurations corresponding to the minimum region.

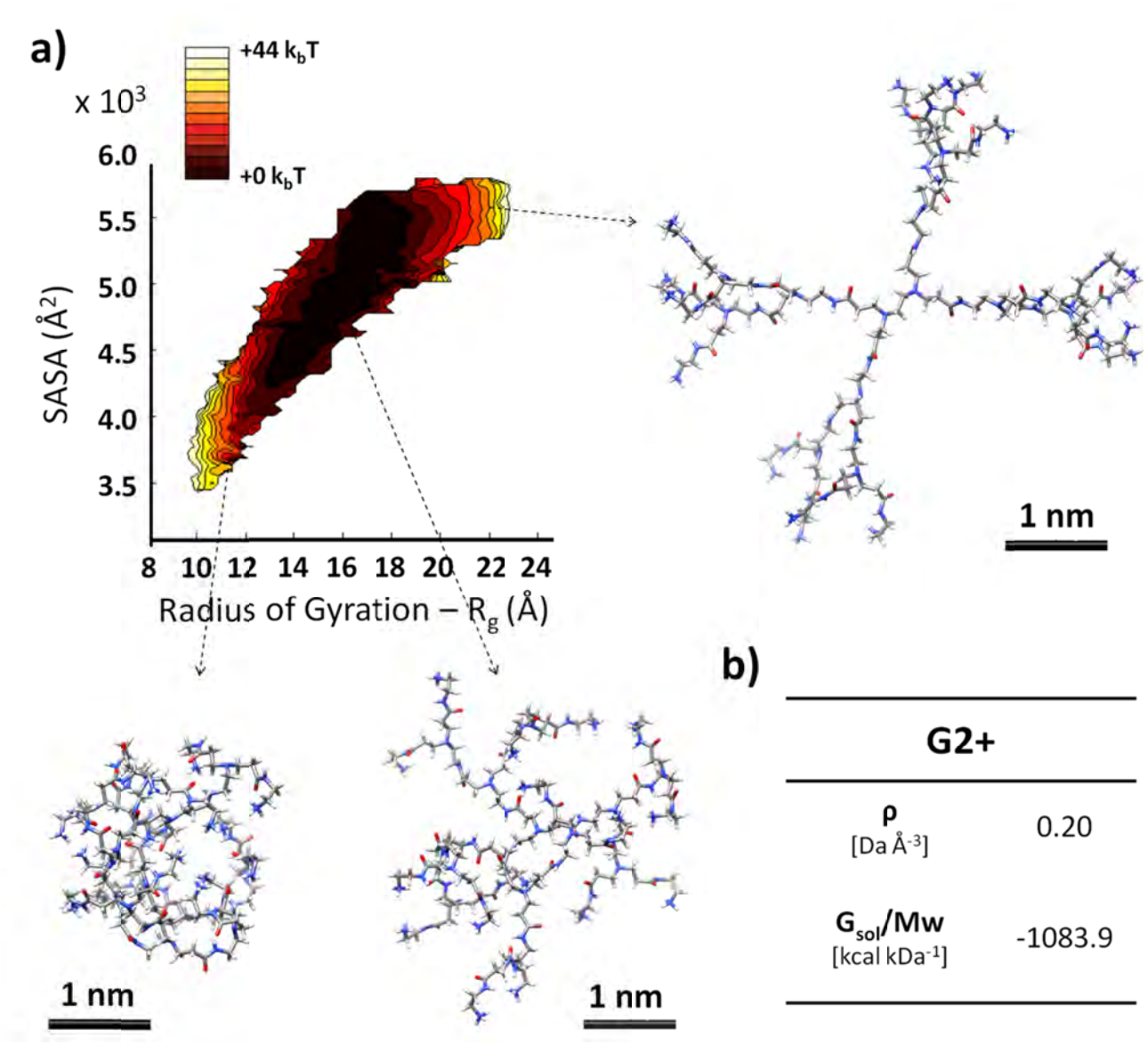

Figure S3. free energy surfaces (FES) of **G2+** (a) obtained from WT-MetaT simulations and calculated respect solvent accessible surface area (SASA – *y* axis) and radius of gyration (R_g – *x* axis). Isolines identify free energy differences of 4 k_bT. The darkest the FES region are the most energetically accessible, and are representative of the most probable molecular configurations. The

dendrimer is colored by atom (C: grey, O: red, N: blue and H: white). Explicit water molecules and Cl^- and Na^+ ions are not shown for clarity. Density and solvation energy data for **G2+** for the configurations corresponding to the minimum region.

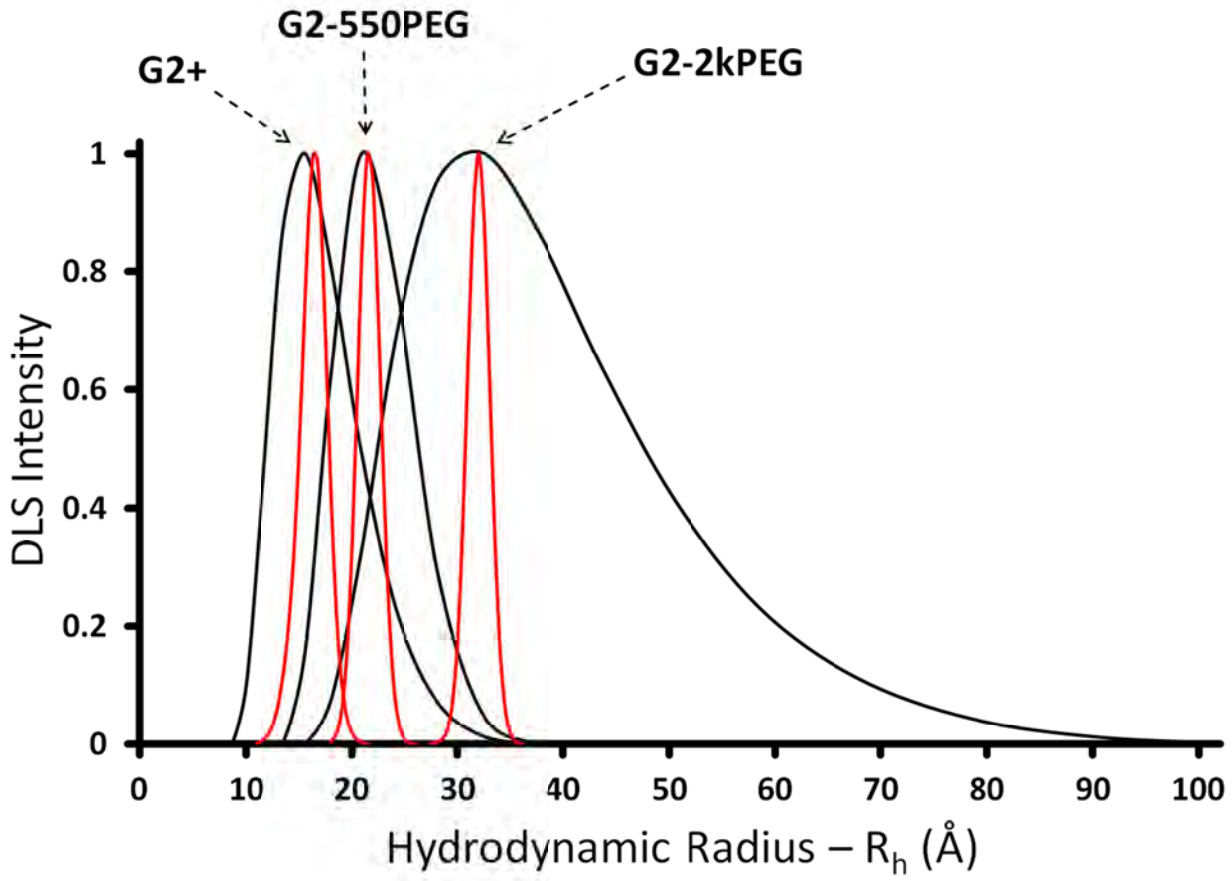

Figure S4. Hydrodynamic radius (R_h) data of the G2+ dendrimer (left peaks) obtained from dynamic light scattering (DLS) experiments (black) and WT-MetaD simulation (red). **G2-550PEG** and **G2-2kPEG** data are reported for comparison.

Additional DLS data

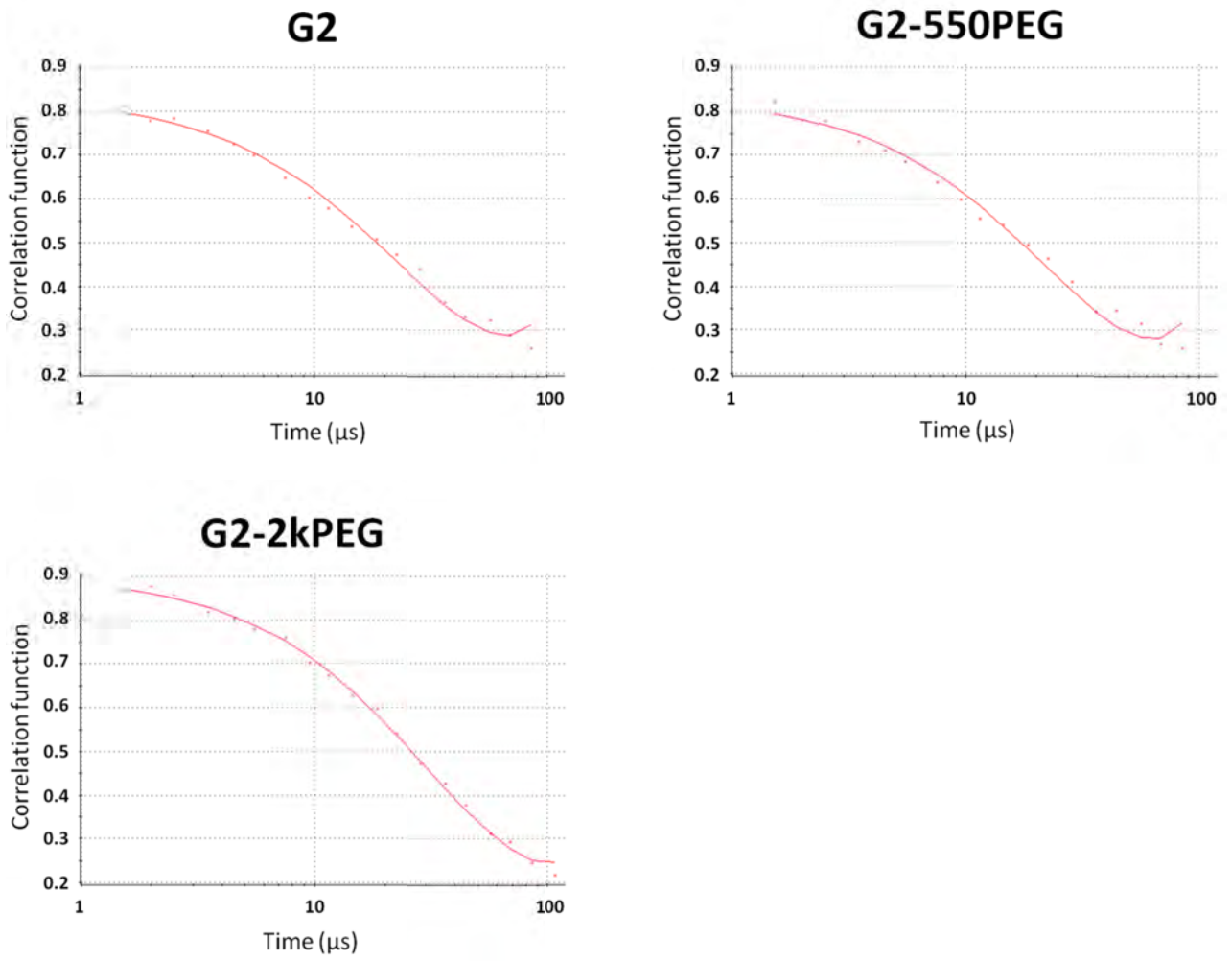

Figure S5. Autocorrelation curves with cumulant method fit for the DLS measurements.

References

S1. Case, D. A.; Darden, T. A.; Cheatham III, T. E.; Simmerling, C. L.; Wang, J.; Duke, R. E.; Luo, R.; Walker, R. C.; Zhang, W.; Merz, K. M.; Robertson, B..; Wang, B.; Hayik, S.; Roitberg, A.; Seabra, G.; Kolossvary, I.; Wong, K. F.; Paesani, F.; Vanicek, J.; Liu, J.; Wu, X.; Brozell, S.; Steinbrecher, T.; Gohlke, H.; Cai, Q.; Ye, X.; Wang, J.; Hsieh, M.-J.; Cui, G.; Roe, D.R.; Mathews,

D.H.; Seetin, M.G.; Sangui, C.; Babin, V.; Luchko, T.; Gusarov, S.; Kovalenko, A.; Kollman, P. A., AMBER 11. University of California, San Francisco, **2010**.

S2. a) Garzoni, M.; Cheval, N.; Fahmi, A.; Danani, A.; Pavan, G. M. *J. Am. Chem. Soc.*, **2012**, *134*, 2249-3357; b) Lim, J.; Pavan, G. M; Annunziata, O.; Simanek, E. E. *J. Am. Chem. Soc.*, **2012**, *134*, 1492-1495; c) Pavan, G. M.; Mintzer, M. A.; Simanek, E. E.; Merkel, O. M.; Kissel, T.; Danani, A. *Biomacromolecules*, **2010**, 11, 721–730; d) Pavan, G. M.; Albertazzi, L.; Danani, A. *J. Phys. Chem. B.*, **2010**, 114, 2667-2675; e) Jensen, L. B.; Mortensen, K.; Pavan, G. M.; Kasimova, M. R.; Jensen, D. K.; Gadzhyeva, V.; Nielsen, H. M.; Foged C. *Biomacromolecules*, **2010**, *11*, 3571-3577; f) Shema-Mirachi, M.; Pavan, G. M.; Danani, A.; Lemcoff, N. G. *J. Am. Chem. Soc.*, **2011**, *133*, 14359-14367.

S3. Albertazzi, L.; Brondi, M.; Pavan, G. M.; Sato, S. S.; Signore, G.; Storti, B.; Ratto, G. M.; Beltram, F. *PLoS One* **2011**, *6*, e28450.

S4. a) Kasimova, A. O.; Pavan, G. M.; Danani, A.; Mondon, K.; Cristiani, A.; Scapozza, L.; Gurny, R.; Moeller, M. *J. Phys. Chem. B*, **2012**, *116*, 4338–45; b) Lim, J; Lo, S.-T.; Pavan, G. M.; Sun, X.; Simanek, E. E. *Mol. Pharmaceutics* **2012**, *9*, 404-412.

S5. a) Doni, G.; Kostiainen, M. A.; Danani, A.; Pavan, G. M. *Nano Lett.*, **2011**, *11*, 723-728; b) Pavan, G. M.; Danani, A.; Pricl, S.; Smith, D. K. *J. Am. Chem. Soc.*, **2009**, *131*, 9686-9694; c) Pavan, G. M.; Kostiainen, M. A.; Danani, A. *J. Phys. Chem. B.*, **2010**, 114, 5686–5693.

S6. a) Jakalian, A.; Bush, B. L.; Jack, D. B.; Bayly, C. I. *J. Comput. Chem.*, **2000**, *21***,** 132-146; b) Jakalian, A.; Jack, D. B.; Bayly, C. I. *J. Comput. Chem.*, **2002**, *25***,** 1623-1641.

S7. Wang, J.; Wang, W.; Kollman, P.A.; Case, D.A. *J. Mol. Graphics Model.*, **2006**, *25***,** 247-260.

S8. Wang, J.; Wolf, R. M.; Caldwell, J. W.; Kollman, P. A.; Case, D. A. *J. Comput. Chem.*, **2004**, *25***,** 1157-1174.

S9. Jorgensen W. L.; Chandrasekhar, J.; Madura, J. D.; Impey, R. W.; Klein, M. L. *J. Chem. Phys.*, **1983**, *79*, 926–35.

S10. Cornell, W. D.; Cieplak, P.; Bayly, C. I.; Gould, I. R.; Merz, K. M.; Ferguson, D. M.; Spellmeyer, D. C.; Fox, T.; Caldwell, J. W.; Kollman, P. A. *J. Am. Chem. Soc.*, **1995**, *117*, 5179-5197.

S11. Barducci, A.; Bussi, G.; Parrinello, M. *Phys. Rev. Lett.* **2008**, *100*, 020603.

S12. Phillips, J. C.; Braun, R.; Wang, W.; Gumbart, J.; Tajkhorshid, E.; Villa, E.; Chipot, C.; Skeel, R. D.; Kale, L.; Schulten, K. *J. Comput. Chem.* **2005**, *26*, 1781-802.

S13. Bonomi, M.; Branduardi, D.; Bussi, G.; Camilloni, C.; Provasi, D.; Raiteri, P.; Donadio, D.; Marinelli, F.; Pietrucci, F.; Broglia, R. A.; Parrinello, M. *Comp. Phys. Comm.* **2009**, *180*, 1961.

S14. Darden, T.; York, D.; Pedersen, L. *J. Chem. Phys.*, **1998**, *98*, 10089-10092.

S15. Andersen, H. C. *J. Comput. Phys.*, **1983**, *52*, 24–34.

S16. a) Bonomi, M.; Barducci, A.; Parrinello, M. *J. Comput. Chem.* **2009**, *30*, 1615-21; b) Barducci, A.; Bonomi, M.; Parrinello, M. *Biophysical J.* **2010**, *98*, L44-L46.

S17. Humphrey, W.; Dalke, A.; Schulten, K. *J. Molec. Graphics* **1996**, *14*, 33-38.

S18. Srinivasan, J.; Cheatham, T. E.Cieplak, P.; Kollman, P. A.; Case, D. A. *J. Am. Chem. Soc.* **1998**, *120*, 9401-09.

S19. Jayaram, B.; Sprous, D.; Beveridge, D. L.; *J. Phys. Chem.* **1998**, *102*, 9571-9576.

S20. Sitkoff, D.; Sharp, K. A.; Honig, B. *J. Phys. Chem*. **1994**, *98*, 1978-1988.

S21. Luo, R.; David, L.; Gilson. M. K. *J. Comput. Chem*. **2002**, *23*, 1244-1253.

S22. Sanner, M. F.; Olson, A. J.; Spehner, J. C. *Biopolymers*. **1996**, *38*, 305-20.